

# Spectral analysis of inhomogeneous network models $\mbox{\it Malhotra}, \mbox{\it N}.$

#### Citation

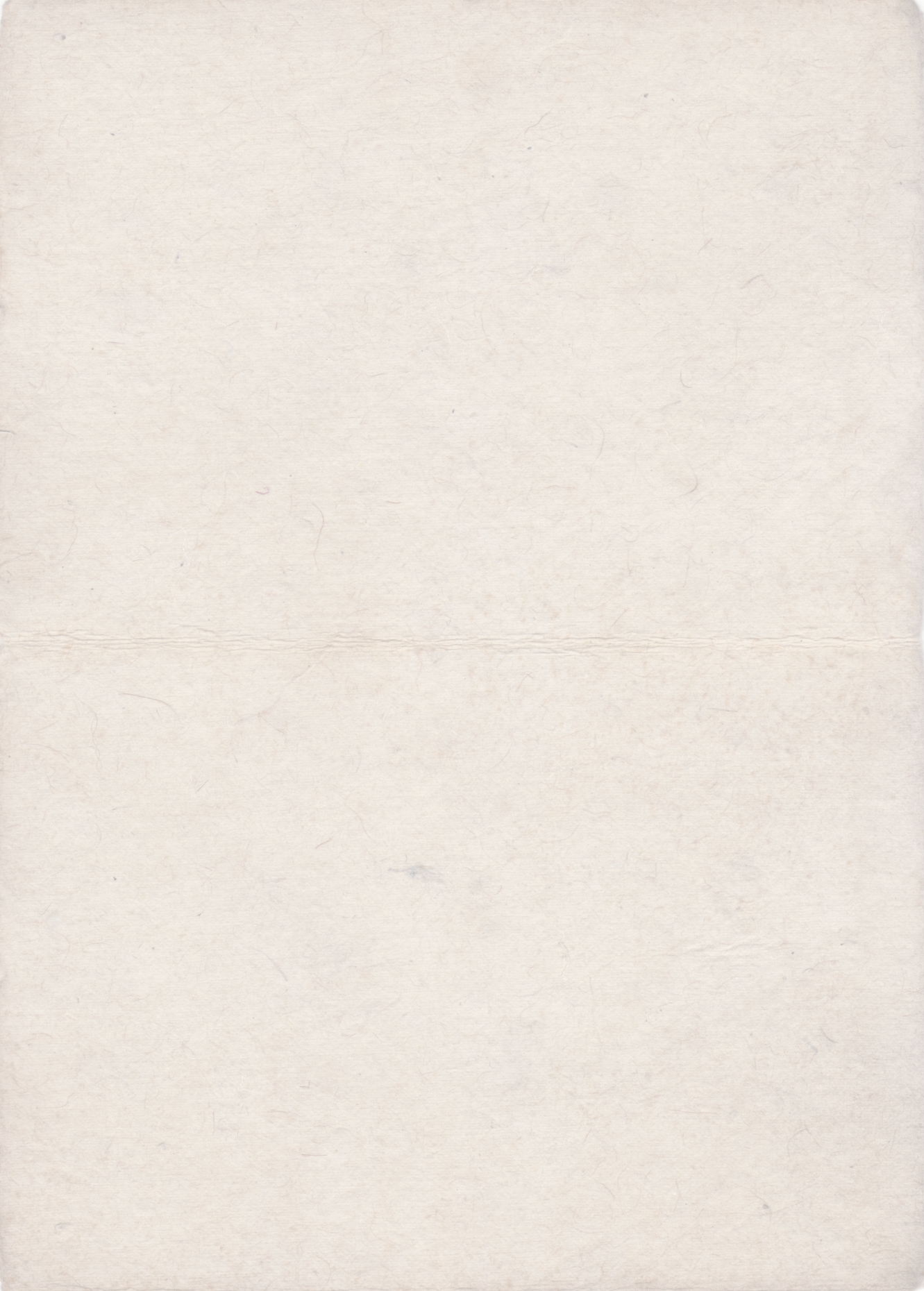
Malhotra, N. (2025, November 20). *Spectral analysis of inhomogeneous network models*. Retrieved from https://hdl.handle.net/1887/4283482

Version: Publisher's Version

License: License agreement concerning inclusion of doctoral thesis in the Institutional Repository of the University of Leiden

Downloaded from: <a href="https://hdl.handle.net/1887/4283482">https://hdl.handle.net/1887/4283482</a>

**Note:** To cite this publication please use the final published version (if applicable).



# Discussion and future directions

In this short chapter, we show some simulations of spectral distributions of random graph models discussed in the previous chapters. We focus on the cases not covered by our main results and compare them with the previous simulations. This leaves us with many open directions for the future.

#### §5.1 Introduction

This thesis establishes new results in the study of spectral analysis of inhomogeneous random graph models, providing further insight into the area and opening the door to multiple directions for further research. We discuss some of the open directions in this chapter.

Chapter 2 extends results of the homogeneous Erdős-Rényi random graph to the inhomogeneous setting, providing a characterisation of the limiting spectral measure of the adjacency matrix. While the limit is not explicitly known, we provide a combinatorial expression for the moments and an analytic description of the Stieltjes transform, which complements the random graph description that one can obtain from Bordenave and Lelarge [2010], since the model has a local weak limit that is a multi-type branching process (see van der Hofstad [2024]). However, the results are restricted to the setting where vertex weights  $(w_i)$  are deterministic, and a natural extension would be to consider random weights with f an almost surely continuous connectivity function. As seen in Remark 2.3.13, our proof techniques require that W (which is the random variable such that  $w_{o_N} \stackrel{d}{\to} W$ ) is compactly supported. What also remains unknown is the rate of convergence of the measure  $\mu_{\lambda}$  to  $\mu_{f}$ , even in the homogeneous setting where  $\mu_f = \mu_{sc}$ . These questions naturally arise due to the works of Bai and Silverstein [2010], Augeri [2025], Jung and Lee [2018], Tran et al. [2013], however, we believe that the fixed-point equation as in Theorem 2.3.9 needs further analysis to describe the rate of convergence of Stieltjes transforms. Furthermore, the extension of results from Bordenave et al. [2011], Coste and Salez [2021], Salez [2020] remains an open question in the inhomogeneous setting.

Spectral properties of kernel-based random graphs (as introduced in Jorritsma et al. [2023]), and in particular of the scale-free percolation model, are a relatively untouched topic. Chapters 3 and 4 now provide a foundation for this topic. We consider random Pareto weights on the vertices, with tail exponent  $\tau - 1$ ,  $\tau > 1$ . The spectral properties of the adjacency matrix are described in Chapter 3 for kernel-based random graphs with the kernel structure

$$\kappa(x,y) = (x \vee y)(x \wedge y)^{\sigma}$$

where  $\sigma < \tau - 2$ . One extension would be to consider a far more general kernel. The above multiplicative structure simplifies calculations significantly. We also restrict ourselves to  $\tau > 2$ , where the weights have finite mean. This is crucial in the truncation step, since for a truncation at m > 1, the error rate is  $m^{2-\tau}$ . We believe that this is a technical assumption. Analogously, we do not consider  $\sigma \ge \tau - 1$ . Due to the rank one nature of the kernel when  $\sigma = 1$ , we can characterise the limiting measure using tools from free probability.

Consequently, we observe an interesting tail asymptotic, where the measure has a power-law tail with exponent  $2(\tau - 1)$ . When  $\sigma \neq 1$ , this becomes more challenging, and we believe that the tail may not have a power-law decay but rather a more complicated behaviour. A more interesting direction is the case when  $\alpha > 1$ , with  $\tau > 2$ . This yields a sparse random graph, for which the existence of a limiting measure is guaranteed by Bordenave and Lelarge [2010]. However, since the local weak limit of the random graph is not locally tree-like, there is no description of the measure. This will require a novel approach, and the spectrum of the centred and non-centred adjacency matrices will differ.

The Laplacian matrix of the scale-free percolation model is analysed in Chapter 4. The existence of the limiting measure is achieved by computing the moments, which is far more challenging than computing the moments of the adjacency matrix. We believe that this will be the primary challenge when attempting to extend the results to the kernel as described in Chapter 3. We also restrict ourselves to  $\tau > 3$ , and an extension to  $\tau > 2$  will require better bounds in the Gaussianisation step, as well as ensuring that the decoupling of the diagonal holds. Decoupling is an essential step for the moment method, without which the approach becomes highly complicated.

#### Outline of the chapter

The first part of the chapter is devoted to the homogeneous Erdős-Rényi random graph  $\text{ER}_N(p)$  with  $p = \lambda/N$ . We simulate the spectrum of the adjacency matrix for increasing  $\lambda$  to illustrate that, for a  $\lambda$  such that  $1 < \lambda < \log N$ ,  $\mu_{\lambda}$  starts taking the shape of  $\mu_{sc}$  (with possible atoms). We then simulate the spectrum of the Laplacian matrix, moving from the sparse to the dense case, and show why centring becomes essential as the graph becomes more dense.

The second part of the chapter showcases simulations for the scale-free percolation model. We simulate the spectra of the adjacency matrix for a combination of  $\alpha$  and  $\tau$ , to analyse the cases where  $\alpha(\tau-1)>1$  and  $\alpha(\tau-1)<1$ . We also simulate the spectrum of the long-range percolation model with increasing  $\alpha$ , to illustrate the sparse setting. We compare the resolvent matrices of the long-range percolation model, GOE model, and  $\text{ER}_N(\lambda/N)$  with  $\lambda>1$ . We conclude with the centred Laplacian matrix of the scale-free percolation model for varying  $\tau$ , namely the infinite mean regime, the infinite variance regime, and the finite variance regime.

## §5.2 Erdős-Rényi Random graph

Consider the homogeneous Erdős-Rényi random graph  $\mathrm{ER}_N(p)$  on N vertices, with  $p = \lambda/N$  for some  $\lambda \in (0, \infty)$ . If  $\mathbf{A}_{\mathbb{G}_N}$  is the adjacency matrix of this graph, then define  $\mathbf{A}_N = \lambda^{-1/2} \mathbf{A}_{\mathbb{G}_N}$  as the scaled adjacency matrix. This

falls under the setting of Chapter 2 as a special case. In particular, Theorem 2.3.7 (and also results from Jung and Lee [2018], Bordenave and Lelarge [2010], Tran et al. [2013]) tells us that there exists a unique limiting measure  $\mu_{\lambda}$  such that  $\lim_{N\to\infty} \mathrm{ESD}(\mathbf{A}_N) = \mu_{\lambda}$  in probability, and  $\mu_{\lambda} \Longrightarrow \mu_{sc}$  as  $\lambda \to \infty$ . Further, from Bordenave and Lelarge [2010], if  $\mathbf{\Delta}_N$  is the scaled Laplacian matrix of this graph, then there exists a unique limiting measure  $\nu_{\lambda}$  such that  $\lim_{N\to\infty} \mathrm{ESD}(\mathbf{\Delta}_N) = \nu_{\lambda}$  in probability. It follows from Khorunzhy et al. [2004] that  $\nu_{\lambda} \Longrightarrow \mu_{sc} \boxplus \mu_q$ , where  $\mu_q$  is the Gaussian law.

#### §5.2.1 Adjacency matrix

Consider the scaled adjacency matrix  $\mathbf{A}_N$  of this graph. In Chapter 2, we see that in the limit  $N \to \infty$ , the ESD of  $\mathbf{A}_N$  and that of the centred matrix  $\mathbf{A}_N - \mathbb{E}[\mathbf{A}_N]$  are close in probability, and so we can study the non-centred matrix directly.

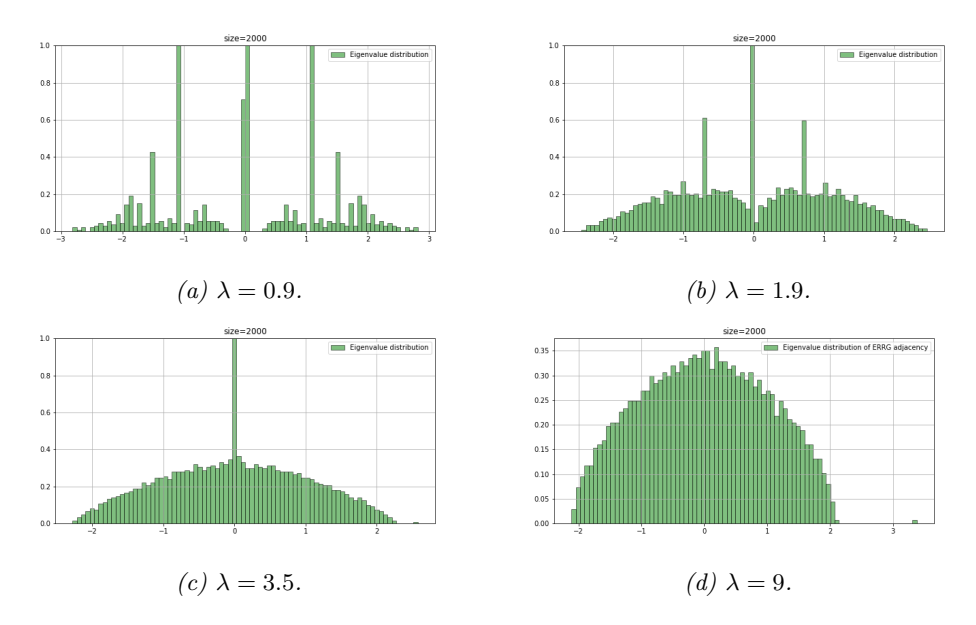


Figure 5.1: Eigenvalue distributions of the adjacency of  $ER_N(\lambda/N)$  with N=2000.

In Figure 5.1, we see the eigenvalue distributions of this matrix with N=2000 for varying values of  $\lambda$ . For  $\lambda<1$ , we observe "spikes", indicating that the measure has many atoms (in line with Salez [2020]). For  $\lambda>1$ , we observe a continuous part, indicating the presence of a density (in line with Arras and Bordenave [2023]). When  $\lambda>\log N$  ( $\lambda=9$ ), we observe a distribution that resembles the semicircle law, with an outlier that is the largest eigenvalue, which is of the order  $\sqrt{\lambda}$  (see Erdős et al. [2013]).

The interesting case is when  $\lambda$  is "large", but smaller than  $\log N$ . We observe at  $\lambda=3.5$  for N=2000 that there is a spike at the eigenvalue 0, indicating the presence of an atom. However, the remaining distribution begins to take the shape of a semicircle distribution. This indicates that the rate of convergence in  $\lambda$  is relatively fast. While we were not able to prove this, we believe that the metric defined by Stieltjes transforms as in Augeri [2025] can aid in determining this rate of convergence. Through moments, we heuristically see a possible candidate for the convergence rate. The 2k-th moment of  $\mu_{\lambda}$  is

$$\int_{\mathbb{R}} x^{2k} \mu_{\lambda}(\mathrm{d} x) = C_k + \mathrm{Err}(\lambda^{-1}) = \int_{\mathbb{R}} x^{2k} \mu_{sc}(\mathrm{d} x) + \mathrm{Err}(\lambda^{-1}),$$

where  $\operatorname{Err}(\lambda^{-1})$  is an error term with leading order  $\lambda^{-1}$  and  $C_k$  is the k-th Catalan number. We leave the optimal rate of convergence as an open problem.

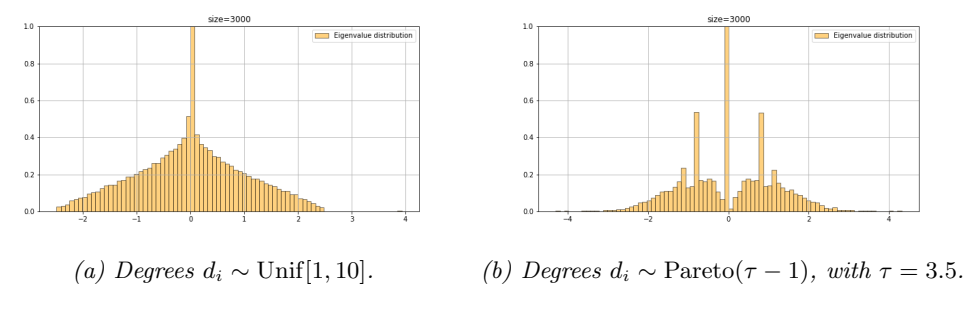


Figure 5.2: Spectral distributions of adjacency matrices of IER models, with edge probability  $p_{ij} = \frac{d_i d_j}{m_1 + d_i d_j} \wedge 1$ , where  $(d_i)_{i=1}^N$  is a given degree sequence and  $m_1 = \sum_{i=1}^N d_i$ . N = 3000.

#### §5.2.2 Laplacian matrix

From Bordenave and Lelarge [2010], we have the existence of  $\nu_{\lambda}$  for the ESD of the graph Laplacian when the graph is sparse. We see in Figure 5.3 that the spectra of the centred and non-centred Laplacian differ significantly, in particular when the sparsity parameter increases. For dense graphs with a fixed p, the spectrum of the Laplacian is a Dirac mass at p (see Bryc et al. [2006]), which is what we observe in Figure 5.3c. It is only meaningful to study the spectrum of the centred Laplacian in the dense setting. Understanding the ESD and identifying the limiting measure in the general inhomogeneous setting is still an open problem. Also, it is unclear whether for any  $\lambda > 0$ , the limiting measure always has an absolutely continuous spectrum. It would be interesting to derive the behaviour of the atoms for  $\lambda < 1$ .

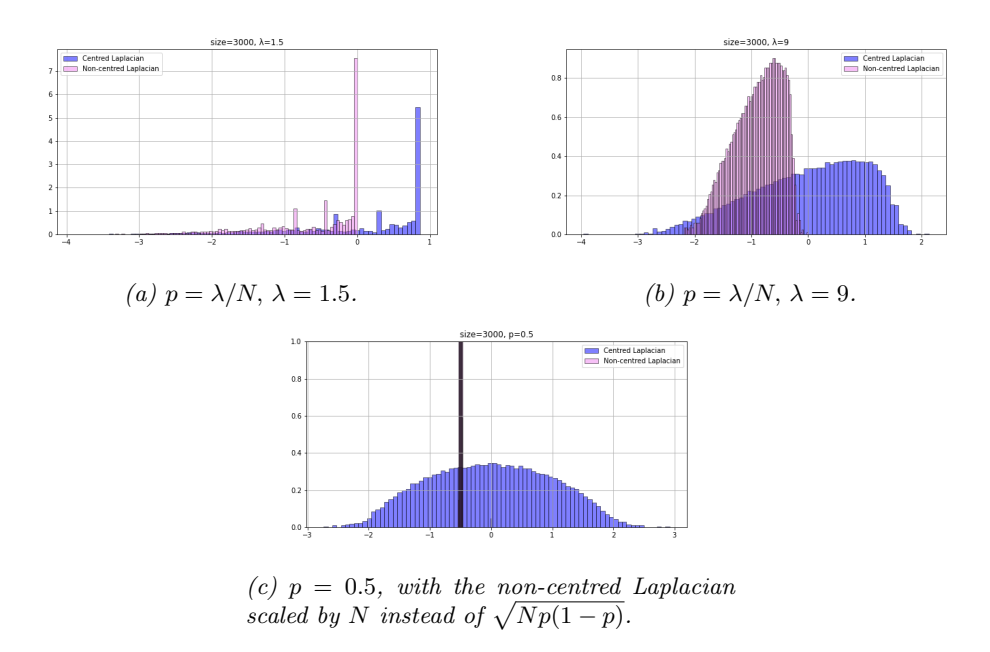


Figure 5.3: Spectral distributions of the Laplacian matrices of ERRG, with N = 3000.

#### §5.3 Scale-Free percolation

Let us consider the model from Chapter 4, which is a special case of the model from Chapter 3. We take the discrete torus on N vertices and an i.i.d. sequence of Pareto weights  $(W_i)_{i=1}^N$ . Conditionally on the weights, we add edges independently with probability

$$p_{ij} = \frac{W_i W_j}{\|i - j\|^{\alpha}} \wedge 1,$$

where  $\alpha > 0$  is a parameter of choice and  $\|\cdot\|$  is the torus distance. In the dense case, we scale the adjacency and Laplacian matrices with the scaling factor  $c_N \sim N^{1-\alpha}$  for  $\alpha < 1$ . In the sparse case, when  $\alpha > 1$ , we scale by a constant scaling  $\zeta(\alpha)$ , which is the Riemann-Zeta function evaluated at  $\alpha$ .

### §5.3.1 Adjacency matrix

The degrees of vertices in the model are heavy-tailed with parameter  $\gamma := \alpha(\tau - 1)$  (see Deijfen et al. [2013], Cipriani and Salvi [2024]). We simulate the eigenvalue distribution of the scaled adjacency matrix  $\mathbf{A}_N$  for the regimes  $\gamma < 1$  and  $\gamma > 1$ . For  $\gamma > 1$ , we have two sub-regimes, namely when  $\alpha < 1$  and  $\alpha > 1$ , and similarly for  $\gamma < 1$ , giving us a total of 4 regimes, as in Figure 5.4. While we have theoretical results for Figure 5.4a, wherein we also see that the centred and

non-centred adjacency matrices are spectrally close, we believe extension to the setting simulated in Figure 5.4b should be possible with some modifications to deal with infinite-mean weights, though the spectrum may differ in the centred and non-centred cases. The eigenvalue distributions in Figures 5.4a and 5.4c look similar, where the parameter  $\gamma>1$ . Similarly, the eigenvalue distribution in Figures 5.4b and 5.4d have a similar shape, where  $\gamma<1$ . This indicates that  $\gamma$  possibly plays a role in the limiting spectrum, though we do not see this in Chapters 3 and 4. We believe that the limiting measures exist in all regimes after appropriate scaling and may be random in certain cases.

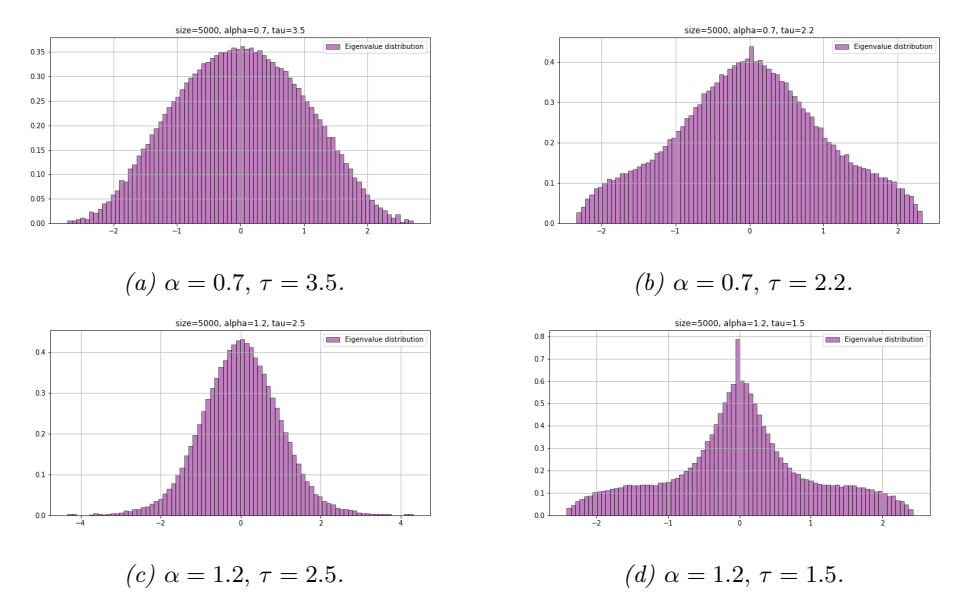


Figure 5.4: Spectral distributions of the centred adjacency matrices of scale-free percolation, with N=5000.

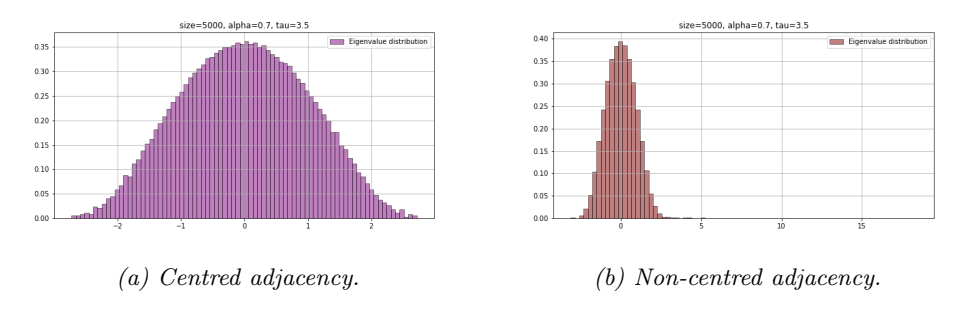


Figure 5.5: Spectral distributions of the centred and non-centred adjacency matrices of scale-free percolation, with N=5000,  $\alpha=0.7$ ,  $\tau=3.5$ .

For the long-range percolation model (that is, for  $W_i \equiv 1$ ) in Figure 5.6, we observe the semicircle law when  $\alpha < 1$ . At  $\alpha = 1$ , the shape is still semicircle-like, though we observe some concentration towards the centre. For  $\alpha \in (1,2)$ , we still observe the presence of a density, with possible atoms at 0, and  $\alpha = 2$ , this density begins to break down. For  $\alpha > 2$ , where the model behaves similarly to bond percolation, the spectrum starts to break down. Such transitions in forms of percolative behaviour in different regimes have already been observed in long-range percolation theory (Berger [2002]). It would be interesting to see this behaviour in the spectrum also.

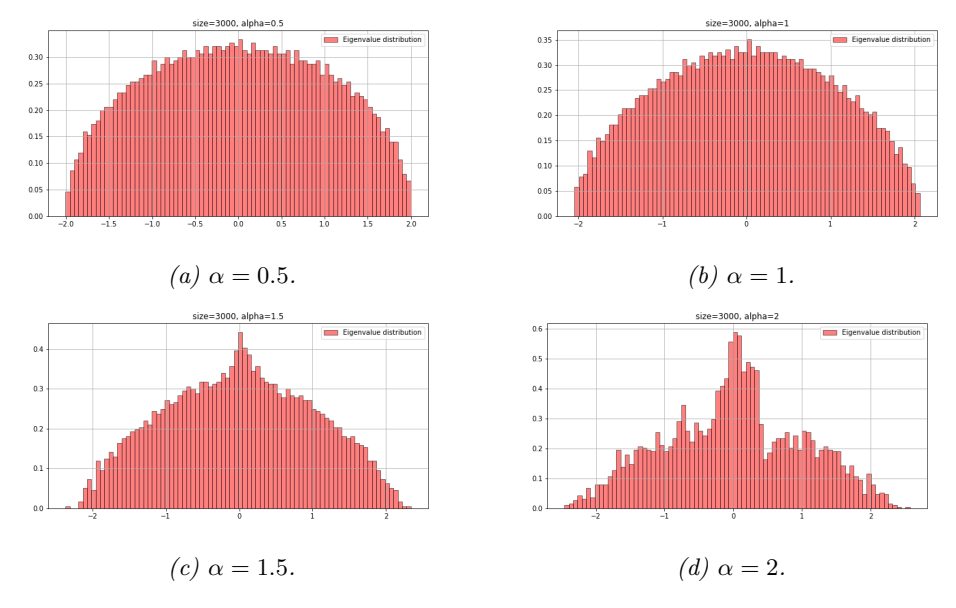


Figure 5.6: Spectral distributions of the centred adjacency matrices of long-range percolation, with N=3000.

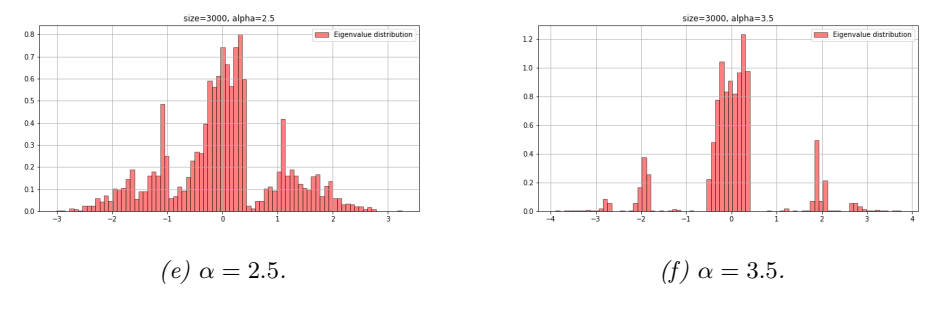


Figure 5.6: (continued)

#### §5.3.2 Resolvent Matrix

Recall that for a random matrix  $\mathbf{A}_N$ , one can define the resolvent as  $\mathbf{R}_{\mathbf{A}_N}(z) = (\mathbf{A}_N - z\,\mathbf{I})^{-1}$ . For some models, there is a concentration on the diagonal of the resolvent matrix, which makes computation easier. For example, let  $\mathbf{A}_N$  be the GOE, with  $\mathbf{A}_N(i,j) = \mathbf{A}_N(j,i) \stackrel{d}{=} N^{-1/2} \mathbf{N}(0,1)$ . With the following heuristic, we can see how concentration on the diagonal of the resolvent occurs:

With Schur's complement formula from Bordenave [2019], we have

$$r_{ii} = -\frac{1}{z + \sum_{j,k \neq i} \tilde{r}_{jk} \mathbf{A}_N(i,j) \mathbf{A}_N(i,k)},$$

where  $\tilde{r}_{ij} := R_{\mathbf{A}_N^{(i)}}(z) = (\mathbf{A}_N^{(i)} - z \mathbf{I})^{-1}$ , and  $\mathbf{A}_N^{(i)}$  is  $\mathbf{A}_N$  with the *i*-th row and column deleted. We briefly recall the heuristics from Chapter 2.1. Taking expectation, we get

$$\begin{split} \mathbb{E}[r_{ii}] &= -\mathbb{E}\left[\frac{1}{z + \sum_{j,k \neq i} \tilde{r}_{jk} \mathbf{A}_N(i,j) \mathbf{A}_N(i,k)}\right] \\ &\approx -\frac{1}{z + \mathbb{E}\left[\sum_{j,k \neq i} \tilde{r}_{jk} \mathbf{A}_N(i,j) \mathbf{A}_N(i,k)\right]} \\ &\approx -\frac{1}{z + \mathbb{E}\left[\sum_{j \neq i} r_{jj} \mathbf{A}_N(i,j)^2\right]} = -\frac{1}{z + \operatorname{tr}(\mathbf{R}_{\mathbf{A}_N}(z))} \,, \end{split}$$

and so for N large, the diagonal terms are in some sense "replaced" by the Stieltjes transform of  $\mu_{sc}$ , with the off-diagonal terms vanishing as  $N \to \infty$ .

This concentration may not happen in other models. Notably, in the sparse case of the long-range percolation model, we see that there seems to be significant mass at the off-diagonal terms.

This suggests that understanding the local convergence for these models is a significant challenge, as most methods require a critical understanding of the resolvent matrix, which roughly concentrates around the diagonal for the classical Gaussian models (Anderson et al. [2010], Bordenave [2019]).

#### §5.3.3 Laplacian matrix

For the scaled Laplacian matrix of the scale-free percolation model, we have theoretical results for the existence of a limiting distribution when the weights have finite variance, as in Figure 5.8a. We observe that as  $\tau$  decreases, that is, the weights become more heavy-tailed, the mass at 0 for the measure increases as well, and when we have infinite mean weights, as in Figure 5.8c, there is an

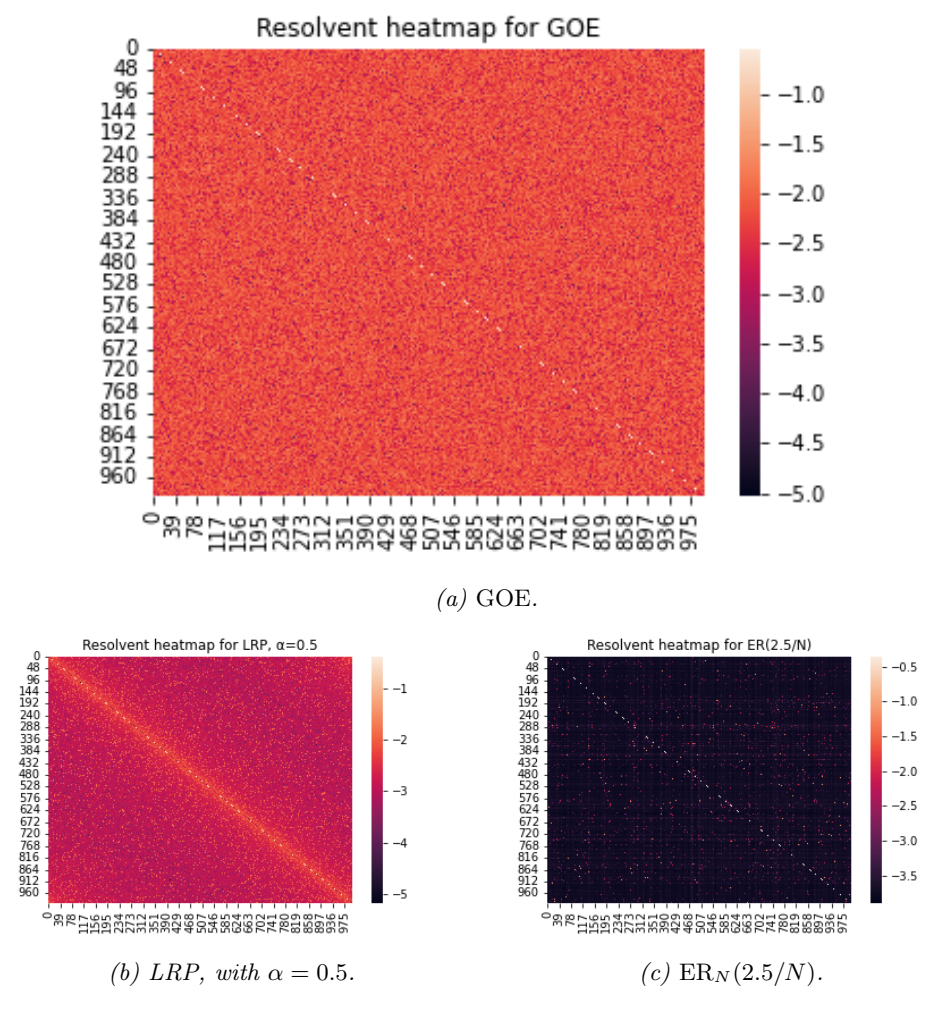


Figure 5.7: Logarithmic resolvent heat maps for centred adjacencies of LRP, GOE, and ERRG models, with N=1000. We take z=1+2i, evaluate the resolvent, and compute the absolute values of the entries. We add  $N^{-2}$  to each entry and compute the logarithm of the value and plot a heat map.

indication of an atom present at 0. We expect the results to be true under the assumption of finite mean for the weights. We remark that the Gaussianisation and decoupling steps may fail when we have infinite variance for the weights, and so, a new approach has to be taken to tackle the problem. We leave the case of finite mean and infinite variance open.

In Figure 5.9, we simulate the eigenvalue distributions of the centred Laplacian matrix of the LRP and SFP models, when  $\alpha > 1$ . We observe that for the LRP, the spectrum breaks down when  $\alpha > 2$ , as in Figure 5.9b, whereas

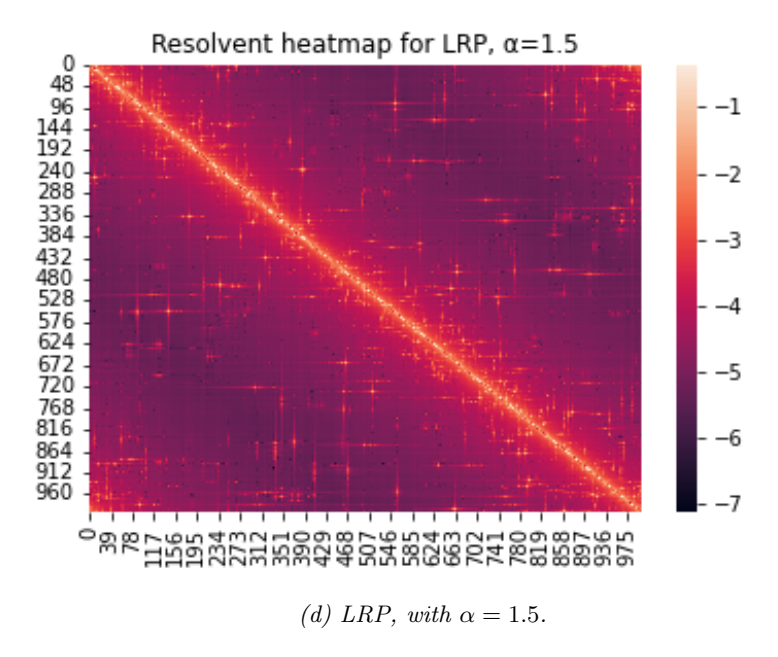


Figure 5.7: (continued)

we observe a density-like shape in Figure 5.9a. For the SFP models, we keep  $\alpha=1.5$  fixed, and observe that the distribution skews less when the weights become more heavy-tailed and the graph becomes denser, as in Figure 5.9d.

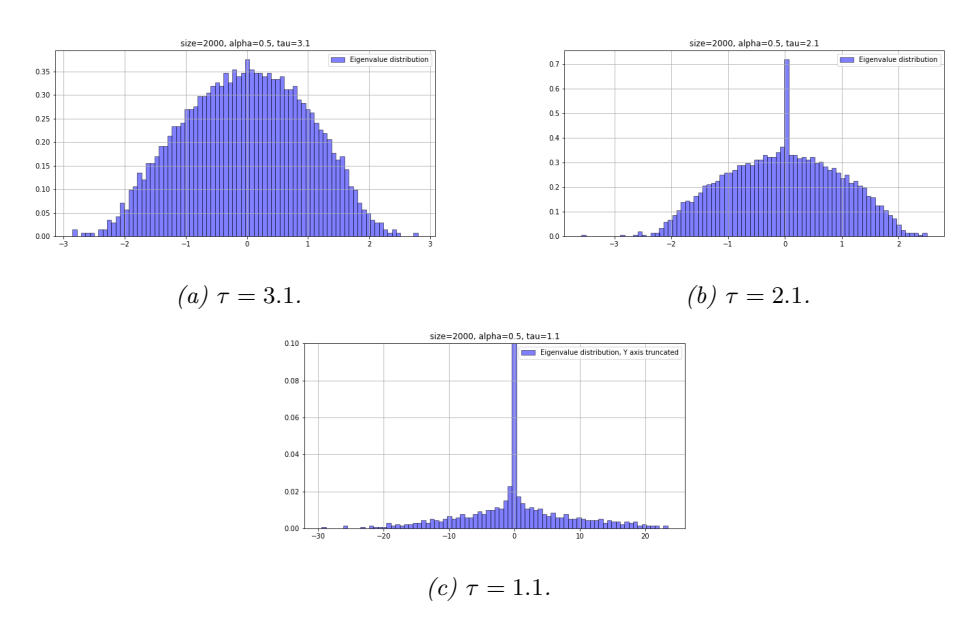


Figure 5.8: Spectral distributions of the centred Laplacian matrix of scale-free percolation, with  $N=2000,\,\alpha=0.5.$ 

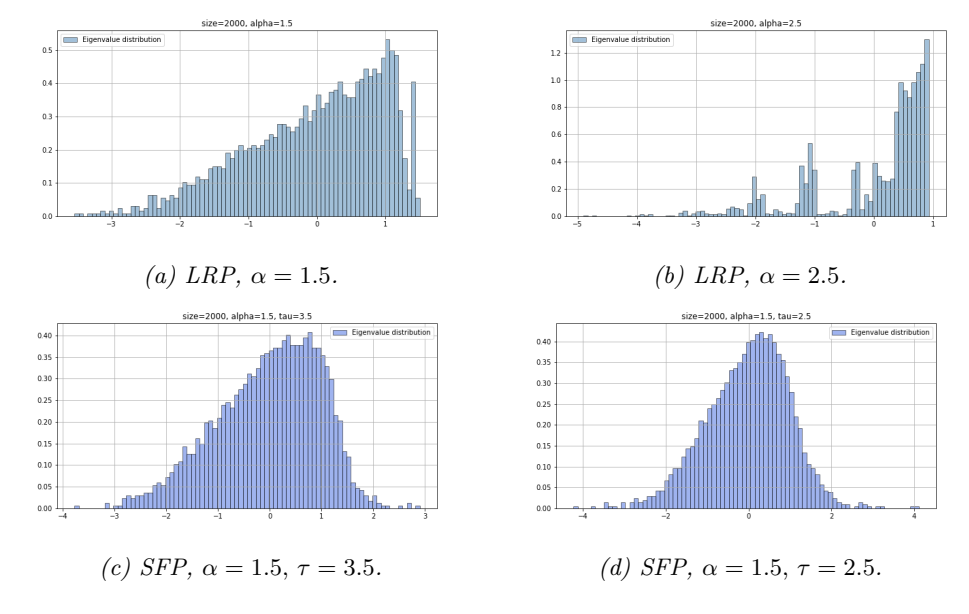


Figure 5.9: Spectral distributions of the centred Laplacian matrix of long-range and scale-free percolation, with N=2000.